Available online at www.sciencedirect.com
ScienceDirect
International Journal of Heat and Mass Transfer 50 (2007) 1938–1952
International Journal of HEAT and MASS TRANSFER
www.elsevier.com/locate/ijhmt

Thermal performance of microencapsulated phase change material slurry in turbulent flow under constant heat flux

Jorge L. Alvarado [a,*], Charles Marsh [b], Chang Sohn [b], Gary Phetteplace [c], Ty Newell [d]

[a] Department of Engineering Technology and Industrial Distribution, Texas A&M University, 117 Thompson Hall, 3367 TAMU, College Station, TX 77843-3367, United States
[b] US Army, Engineer Research and Development Center, Construction Engineering Research Laboratory, 2902 Newmark, Drive, Champaign, IL 61822-1076, United States
[c] US Army, Engineer Research and Development Center, Cold Regions Research and Engineering Laboratory, 72 Lyme Road, Hanover, NH 03755-1290, United States
[d] Mechanical and Industrial Engineering Department, University of Illinois at Urbana-Champaign, 140 Mechanical Engineering Building, 206 West Green Street, Urbana, IL 61801, United States

Received 15 May 2006; received in revised form 29 September 2006
Available online 30 November 2006

Abstract

Current cooling and heating distribution systems that use water as secondary fluid exhibit limited thermal capacity which can only be overcome by high flow rates and large (volume) capacity. A successful way to enhance the thermal capacity of secondary fluid systems is by incorporating microencapsulated phase change material (MPCM) slurry. However, a full understanding of the physical properties and heat transfer characteristics of MPCM slurry in the 2–8 °C range (35.5–46.5 °F) still is lacking. In the paper, latent heat of fusion, melting and freezing points, and temperature- and concentration-dependent viscosity data, are presented. Results indicate that selection of nucleating agent type and concentration is required to prevent the supercooling phenomenon. Pressure drop and convective heat transfer data were measured using a heat transfer loop operated at different flow rates and heat flux values. Results indicate that the phase change process and slurry mass fraction affect the heat transfer process. The paper also examines the impact of using enhanced surface tubing in combination with MPCM slurry under constant heat flux and turbulent conditions.

Keywords: Microencapsulated phase change material slurry; Turbulence; Supercooling; Enhanced surface

1. Introduction

Recently, researchers and engineers have investigated the effects, advantages and disadvantages of incorporating phase change materials in secondary heat transfer fluids with the objective of increasing thermal capacity in district cooling applications. More recently, research has shown that heat capacity in those systems can be increased by fourfold [1]. However, wide implementation of PCM in cooling systems has been limited by several operational factors including clogging of pipes and limited heat transfer rates in heat exchangers [2,3]. Recent developments have demonstrated that microencapsulation of phase change material (MPCM) can be applied to circumvent the problems associated with PCMs. By microencapsulating and isolating the phase change material from its surroundings and the carrier fluid, the phase change material is less likely to hamper the heat transfer process. MPCM slurries have indeed become a viable option for heat transfer processes in recent years. However, MPCMs also host a series of implementation concerns including supercooling, durability, increased pressure drop and limited heat transfer. In the end, the heat transfer effectiveness of any MPCM slurry must be fully characterized and understood to become a fully viable heat transfer fluid.

* Corresponding author. Tel.: +1 979 458 1900; fax: +1 979 862 7969.
E-mail address: alvarado@entc.tamu.edu (J.L. Alvarado).

0017-9310/$ - see front matter © 2006 Elsevier Ltd. All rights reserved.
doi:10.1016/j.ijheatmasstransfer.2006.09.026

Nomenclature

C	heat capacity, kJ/kg
c_p	specific heat, kJ/kg °C
d_p	particle diameter, μm or m
d	pipe or tubing diameter, m or mm
f	Darcy friction factor
g	gravity constant, m/s^2
h	convective heat transfer coefficient, W/m^2 °C or kW/m^2 °C
h_f	head or pipe loss, m
k	thermal conductivity, W/m °C
k^+	dimensionless roughness
k	roughness, m
L	tubing length, m
L_e	characteristic turbulence length scale, m
LHF	latent heat of fusion, kJ/kg
$\dot{m}$	mass flow rate, kg/s
MF	mass fraction
Nu	Nusselt number, hL/k_f
Pr	Prandtl number, $c_p\mu/k$
Pe	Peclet number, RePr
q''_w	wall heat flux, W/m^2
q''	heat flux, W/m^2
R	pipe radius, m
Re	Reynolds number, $Vd\rho/\mu$
Re_p	particle Reynolds number, $Vd_p\rho/\mu$
Ste	Stefan number
th_p	particle thickness, m or μm
T_{bulk}	bulk fluid temperature, °C
T_{wall}	wall temperature, °C
U^*	friction velocity, m/s
V	fluid velocity, m/s
y	particle size, m

Greek symbols

α	heat diffusivity, $k/\rho c_p$
λ	latent heat of fusion, kJ/kg
ε	roughness, m
ϕ	percent of particles migrating to before-melting region
ρ	fluid density, kg/m^3
ν	kinematic viscosity, m^2/s
μ, η	dynamic viscosity, cP or mPa s
τ	fluid shear stress, Pa
ΔP	pressure drop, kPa

Subscripts

B	bulk
MPCM	microencapsulated phase change material
P	particle
W	wall

In this paper, thermophysical properties data of MPCM slurry, including latent heat of fusion, apparent specific heat, melting and crystallization temperature points, and apparent viscosity, are presented. The paper also presents how enhanced surface copper tubing combined with MPCM slurry impact the heat transfer process under constant heat flux and turbulent conditions.

2. Background

2.1. Phase change materials

For several years, research activities have shown that PCMs can enhance the heat capacity of secondary fluids. Researchers have tested paraffins and ice slurries as heat capacity enhancers. Bellas et al. [4] used ice slurries to increase the thermal capacity of an existing system. Choi [3] and others [5–10] have used paraffins because their melting points are at least few degrees greater than the carrier fluid (water). Full implementation of plain PCM in secondary fluid applications has been limited due to the tendency of PCM to form clumps, which exhibit lower thermal conductivity during the solidification process. Also, PCM studies have revealed that higher mass fractions yield higher effective specific heat [3]. However, higher mass fractions also result in higher apparent viscosity, which translates into greater pumping power [3,4,7] and lower thermal conductivity near or on the boundary layer. Choi [3] observed that melted PCM tends to remain near the surface of the heat-conducting pipe while still-solid emulsions remain near the fluid core. Since liquid paraffins have lower thermal conductivity than water, the overall heat transfer process is critically limited which outweighs any coincident enhancements in heat capacity. Despite the use of emulsifiers [3], accumulation of frozen PCM particles on heat exchanger surfaces has been observed, which limits heat transfer. Choi [3] also observed significant changes in pressure drop once the PCM emulsion had melted.

2.2. Microencapsulated phase change material

Few journal articles concerning MPCM physical properties have been published. Roy and Sengupta [11] conducted experimental studies to evaluate the properties of MPCMs with two characteristic thicknesses. Differential scanning calorimetery (DSC) was used to determine the thermal properties. Yamagishi et al. [12] presented experimental results indicating that MPCM particle size does not affect melting temperature and latent heat of fusion. However, the degree of supercooling or the difference between crystallization and melting temperature points increased when particle size, d_p, was less than 100 μm. As a result, Yamagishi et al. [12] also used and tested nucleating agents with molecular structure similar to the PCM

molecules and were able to suppress the supercooling effect considerably. Alvarado [13] conducted a series of experiments and evaluated the thermal properties of tetradecane microcapsules with an average size of 4.4 μm. Yamagishi et al. [2] presented empirical data for microencapsulated octadecane obtained by using DSC equipment, a Couette viscometer [12], and a heat transfer loop [2]. Their results indicate that anionic surfactants can decrease the apparent viscosity of MPCM slurry and turn it into Newtonian-like fluid at high mass fractions (20–30%). The results also indicate that the relative viscosity of the MPCM slurry was independent of temperature. As a result, Yamagishi et al. [2] used the Vand model [14] to predict the relative viscosity of the MPCM slurry at different volume fractions.

Ohtsubo et al. [15] presented experimental data that explained why microcapsules fail structurally. Several experiments show that as d_p/th_p increases, the percentage of broken capsules increases, where d_p and th_p are microcapsule diameter and thickness, respectively.

A limited number of journal articles present and discuss heat transfer and pressure drop data and characteristics for MPCMs. Goel et al. [16] describe experiments of MPCMs filled with *n*-eicosane where the experimental conditions were limited to laminar flow and constant heat flux. Their results indicate that the Stefan number (Ste) was the most dominant parameter, especially for a Ste less than 1.0. Roy and Avanic [17] showed that laminar forced convection heat transfer characteristics for PCM are similar to MPCMs. Based on observations and past research activities, MPCM walls seem not to have a significant impact on the heat transfer process. For MPCM microcapsules (less than 20 μm) filled with *n*-tetradecane, the calculated Biot number is less than 0.1. Results also indicate that the Reynolds number plays a significant role in the heat transfer process. Yamagishi et al. [12] experimental data shows that MPCM slurry approximately follows the Blasius equation. They also conducted several heat transfer experiments with uniform heat flux and turbulent conditions. In their research, MPCM particles were made of octadecane ($C_{18}H_{38}$) which varied in size between 2 and 10 μm. Results show that as mass fraction increases, turbulent flow changes to laminar, which consequently changes the heat transfer characteristics of the MPCM slurry. Unlike the work by Choi [5], no evidence of pressure drop fluctuations can be found when PCM melts within the MPCM particles, and a constant relative viscosity is observed when the slurry temperature increases [12,13]. At high mass fraction, pressure drop decreased, indicating that the slurry became laminarized. One important observation was the effect of particle size on the convective heat transfer coefficient. It is known that particle size [18,19] can either enhance or suppress turbulence which affects momentum and heat transfers. In the case of small MPCM, turbulence is significantly suppressed [2,13]. One significant assumption is that all microcapsules are small, hence, they melt and solidify instantaneously. Experimental data [2,13] suggest that at an identical heat flux, water has a higher h than MPCM slurry. It was concluded that changes and lower values in viscosity promoted turbulence better in water than in MPCM slurry. Yamagishi et al. [2] used Choi's model [3] to predict the local Nusselt number, which is defined as

$$Nu_x = 0.00425 * (Re_{bx}^{0.979} Pr_{bx}^{0.4}) \left(\frac{\eta_{wx}}{\eta_{bx}}\right)^{-0.11} \quad (1)$$

where, Nu_x, Re_{bx}, Pr_{bx}, η_{wx}, and η_{bx} are local Nusselt, local Reynolds, and local Prandtl numbers respectively, and local wall and bulk viscosities, respectively. They observed that Choi's model could be used to predict after-melting behavior (if the single-phase approximation is based on Re_x and Pr_x). However, the model poorly predicted the before- and during-melting Nu_x because the MPCM phase change process affects c_p and h. Experimental data show that higher heating rates yields lower h, which can be attributed to a thicker boundary layer of melted PCM. Data also show that at the same Reynolds number, h increases with mass fraction. It was also evident that higher Reynolds number favors a higher h more than positive changes in mass fraction because higher mass fraction yields higher viscosity and suppressed turbulence. In laminar flow, MPCM benefits are limited because solid and melted microencapsulated PCM segregates around the core fluid [2]. However, recent publications [20,21] based on numerical simulations show that laminar convective heat transfer of MPCM slurries can be enhanced by tweaking several variables including Reynolds number and particle size.

2.3. Enhanced surfaces

Durmus et al. [22] present experimental results where snail-type swirl generators were used to augment heat transfer rates. Results indicate that Nusselt number (Nu) can be increased from 80% to 200% for 15–75° swirling angles for air in a counter-flow configuration, but pressure drop increased by 110%. Performance was better when high swirling angles and low Reynolds numbers were used. Fossa and Tagliafico [23] tested and measured heat transfer rates with and without smooth, finned, grooved pipes which indicate that polymeric additives reduce friction factor but also decrease the Nusselt number. Finned and grooved pipes show a sharper reduction in Nusselt number than smooth pipes for concentrations of 40 ppm and Reynolds number between 7000 and 10,000. Fanning friction factor, f, decreases with respect to pure water only in turbulent flows, by about 25% for finned or grooved pipes and about 20% for smooth pipes. Results also indicate that conductance is greater for finned pipes than for smooth pipes with or without additives. Results also indicate that friction factor reduction reaches a minimum at a specific Reynolds number and additive concentration. Liao and Xin [24] present experimental results on heat transfer and friction characteristics for various liquids with turbulent, transi-

tional, and laminar flow inside a pipe with twisted-tape insert. Results indicate that in turbulent and transitional flows, heat transfer is increased slightly while pressure drop increases significantly. When VG46 turbine oil flow is laminar, the Stanton number is 5.8 times higher when a twisted-tape insert is used instead of a smooth pipe. The friction factor, f, increases 6.5 times also under the same conditions. Stanton number and f with twisted-tape inserts increase with lower tape twist ratio. Segmented twisted-tape inserts can decrease f by 41–44% and Stanton number by 15–18% in relation to a continuous twisted-tape insert.

As seen above, only Yamagishi et al. [2] have brought together some of the issues concerning MPCM. In the next sections, experimental data for microencapsulated tetradecane are presented including pressure drop and heat transfer rates results when smooth and enhanced tubing were used.

3. Physical characterization of microencapsulated tetradecane

3.1. Size characterization

The MPCM used in this study were made by microencapsulating 99% *n*-tetradecane with gelatin through the process of coacervation. The process produces cross-linked microcapsules in the range of 2–260 μm (diameter). Several batches of microencapsulated *n*-tetradecane were prepared to determine the best chemical composition (phase change material and nucleating agent) to minimize the supercooling phenomenon and ensure the long-term durability of the microcapsules, the two main challenges in the design, fabrication and implementation of MPCMs. Table 1a shows the composition and particle size range for the different MPCM slurry batches that were tested.

Each batch was examined under a microscope equipped with a software package capable of measuring particle or microcapsule diameter. Magnifications of 100×, 400× and 1000× were used to determine particle size of each micrograph. Over 300 microcapsules were carefully measured. Fig. 1a shows the particle size distribution of MPCM slurry with the optimal supercooling and durability characteristics.

Alvarado [13] determined that MPCM slurry behaves as a homogeneous fluid based on visual observations. Analysis shows that the total vertical displacement of a 10 μm MPCM particle in a 1.5 m heat transfer section is less 10 μm at a slurry velocity of 0.6 m/s, if gravitational and buoyant forces are taken into account [25]. Also, turbulence promoters were installed and used between each heat transfer section to make sure MPCM particles were uniformly distributed. Therefore, no MPCM particle segregation was observed at slurry velocities equal to or greater than 0.6 m/s.

Table 1a
Characteristic size range of MPCM particles

Batch number	Phase change material	Nucleating agent	MPCM size range (μm)	Average microcapsule diameter (μm)
1	99.8% tetradecane	0.2% fume silica	90–150	100
2	98% tetradecane	2% tetradecanol	70–260	145
3	94% tetradecane	6% tetradecanol	2–10	4.4

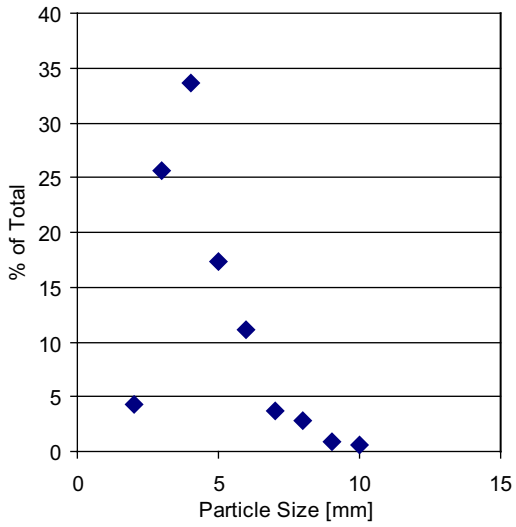

Fig. 1a. MPCM particle size distribution.

3.2. Thermal properties characterization of MPCM slurry by using DSC

A differential scanning calorimeter (DSC) was used to determine the thermal properties of microencapsulated tetradecane, a critical step in the characterization of MPCMs. The DSC measures the amount of heat absorbed or released by a sample in comparison with a standard reference. The resulting energy-temperature curve is used to determine latent heat of fusion and melting point [26–28]. More information on DSC methods and equipment can be found in ASTM E 1269.

A TA Instruments 2920 Modulated Differential Scanning Calorimeter was used to determine the thermal properties of MPCM slurry. Helium gas at a flow rate of 26 cm^3/min was used as purge gas. The DSC was calibrated by performing baseline, cell constant and temperature calibration runs. The information collected from the calibration runs were taken into consideration by the software built into the DSC for computing thermal properties. The built-in software compared the data from the all the calibration runs and determined baseline slope, baseline offset, cell constant values, and temperature corrections. The combined average cell constant value was 1.09, which was used as a correction factor to determine how much energy was actually delivered and received by each specimen. The calibration and experimental runs were

performed by using a heating rate of 3 °C/min for all the experiments. Based on the calibration process, the DSC results are within a 2% relative error. Every MPCM slurry sample was placed in a vial and magnetically stirred to make sure all the particles remained in suspension, before conducting the DSC experiments. Specially designed sealed DSC pans were carefully used and reopened after each DSC test to allow evaporation of the carrier fluid (water) to determine the mass fraction of each sample.

DSC experiments were carried out to measure the latent heat of fusion and melting point of bulk tetradecane with and without nucleating agent. DSC results indicate that 100% bulk tetradecane heat of fusion value and melting and crystallization points are 215 J/g, 5.5 °C and 0.0 °C, respectively. DSC curves and data for bulk tetradecane can be found in Alvarado et al. [29].

To avoid any degree of supercooling (difference between melting and solidification points), a batch of MPCM containing 0.2% of fumed silica as nucleating agent was made. The experimental data show that an average MPCM particle consists of 88.3% of *n*-tetradecane and 11.7% of microcapsule wall material.

Under equilibrium conditions, the melting and crystallization points are identical. However, due to the size of the MPCM particles and finite cooling rates (1–9 °C/min), MPCM particles exhibit a certain degree of supercooling. Supercooling is defined as the difference between freezing (i.e. crystallization) and melting points. DSC experiments clearly show that the degree of supercooling for microencapsulated tetradecane containing 0.2% of fumed silica still is significant and highly undesirable since the carrier fluid is water, whose bulk melting and crystallization points are 0 °C. As a result, considerable amount of effort was undertaken to understand the nature of supercooling in microcapsules. Most knowledge about supercooling is provided by the Classical Nucleation Theory (CNT) and several experimental results published in the past 20 years.

Classical Nucleation Theory asserts that liquid-to-solid transformations take place because of a homogeneous or heterogeneous nucleation mechanism. Homogeneous nucleation relies on the formation and growth of stable nuclei within the microcapsule while heterogeneous nucleation is a surface-mediated mechanism. It is known that homogeneous nucleation has a greater nucleation barrier than heterogeneous nucleation and entails greater supercooling or a lower temperature for stable nuclei to form and grow [30]. Montenegro and Landfester [31] found that nanodroplets (125–500 nm) showed a considerable degree of supercooling, indicating homogeneous nucleation as the preferred type of nucleation mechanism. The most recent experimental data also show that the initiation of freezing temperature does depend on particle size [12,30].

Yamagishi et al. [12] encountered similar difficulties in suppressing supercooling and used paraffin-like molecules with higher melting points than their homologous molecules as nucleating agents. To determine the right amount and type of nucleating agent for microencapsulated tetradecane so the supercooling phenomenon could be controlled effectively, bulk mixtures of tetradecane and tetradecanol at different ratios were tested by using DSC. Fig. 1b shows the DSC results for different concentrations of tetradecanol in tetradecane. In bulk samples, 2% of tetradecanol is sufficient to suppress supercooling almost entirely.

DSC results for MPCM containing 98% tetradecane and 2% tetradecanol (2nd batch) that varied in size between 70 and 260 μm in diameter indicate that the degree of supercooling is considerably less than in the previous case. However, durability test results later indicated that the second batch was unsuitable for further testing. Detailed description of the durability experiments and their results are presented later in the article. Several thermal characterization experiments using DSC were conducted to determine the best combination of phase change material, nucleating agent and microcapsule size. The results of the experiments are presented in Table 1b.

The results shown in Table 1b reiterate previous findings that microcapsule size does have an impact on the phase change material crystallization temperature. However, due to durability problems of larger capsules (over 100 μm),

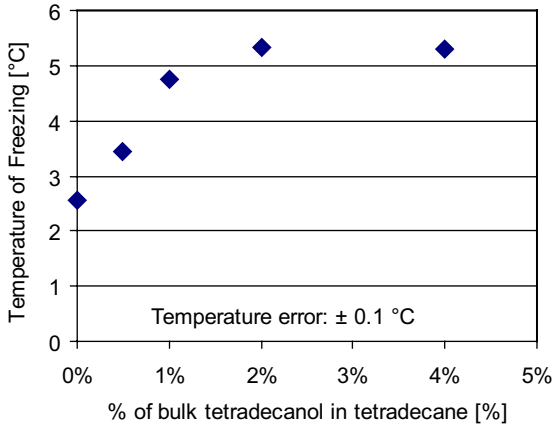

Fig. 1b. Apparent specific heat of MPCM slurry (94% tetradecane + 6% tetradecanol).

Table 1b
DSC results for bulk and microencapsulated tetradecane

Mixture description	T_m (°C)	T_{sol} (°C)	λ (J/g)
Bulk 100% tetradecane	5.5	0	215
Microencapsulated 100% tetradecane	5.2	−4.2	215
Bulk 96% tetradecane + 4% tetradecanol	5.5	5	206.4
Microencapsulated 96% tetradecane + 4% tetradecanol	5.2	2.0	206.4
Bulk 94% tetradecane + 6% tetradecane + 6% tetradecanol	5.5	5	202.1
Microencapsulated 94% tetradecane + 6% tetradecanol	5.1	2.4	202.1

Note: T_m, T_{sol}, λ are melting temperature, crystallization temperature, latent of heat of fusion, respectively. MPCM size range: 2–10 μm.

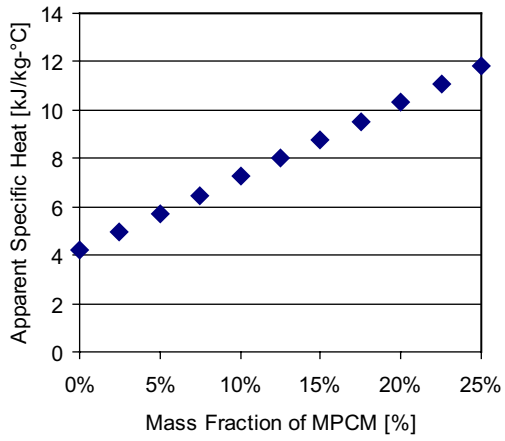

Fig. 1c. Temperature of freezing of tetradecane with tetradecanol as nucleating agent.

microcapsule size should be less than 20 μm to avoid breakage.

To estimate the effect of using MPCM made of 94% tetradecane + 6% tetradecanol in a district cooling application, the apparent specific heat as a function of mass fraction was calculated for a slurry temperature rise of 5 °C, Fig. 1c.

3.3. Durability of MPCM

MPCMs need to withstand continuous pumping and turbulent flow conditions for a considerable amount of time to be able to be used in heat transfer applications. Several batches of MPCM particles were subjected to durability tests. A durability test loop was built and used to determine what percentage of a fixed amount of MPCM slurry could survive continuous pumping and surface friction losses. The durability loop consisted of a closed loop made of copper tubing that varied in diameter from 10.9 mm to 25.4 mm (3/8 to 1 in.). A Moyno progressing cavity pump was used to pump the MPCM slurry through the system because it has shown previously to cause the least damage to MPCM particles and can handle viscous slurries [12]. Periodic samples were taken and analyzed. First, samples were optically examined by using a laboratory-grade microscope with magnifications varying between 40× and 1000× to look for any physical damage. Second, the total amount of released or free tetradecane was determined by using a filtration device that separated the liquid phase (including any free tetradecane) from the solid phase (unbroken microcapsules). If a considerable amount of particles (i.e. 10% or more) broke as a result of durability testing, smaller capsules or capsules with greater thickness-to-diameter ratio were then tested. Ohtsubo et al. [15] showed experimentally that the thickness-to-diameter ratio is the primary variable that predetermines the long-term durability of microcapsules. The objective was to design and test microcapsules with a failure rate of less than 2%. The filtration device used to separate the solid phase from the liquid phase consisted of a 0.2 μm membrane filter and membrane holder. A vacuum line was connected to the discharge side of the membrane holder to speed up the filtration process.

As part of the durability test procedure, different experimental conditions were selected, including slurry velocity and level of turbulence. The slurry velocity ranged between 0.3 m/s (1 ft/s) and 2.44 m/s (8 ft/s), to determine the degree of damage, if any. Three batches of different MPCM size range were tested, and the results are summarized in Table 1c.

The results depicted in Table 1c are consistent with the results published by Yamagishi et al. [12], which also conclude that microcapsule size is the main factor affecting durability. The durability experimental results clearly indicate that small microcapsules (2–10 μm) show the least degree of damage, and therefore are suitable for further experimentation. The results also show that after 1200 circulation times or cycles through the progressing pump (3rd batch), no significant damage on the microcapsules was detected. Also, no perceivable physical damage or deterioration of MPCM thermal properties was detected after the culmination of all the pressure drop and heat transfer experiments.

3.4. Viscosity measurements of MPCM slurry

Past investigations have described and reported on the impact of spherical particles on the apparent viscosity of slurries. Vand [14] carefully studied the interactions among particles in liquids, and proposed a model, which has been regarded as the basis for the study of slurry viscosity. Thomas [32] also studied in detail and proposed viscosity models for dilute and concentrated suspensions. Yamagishi et al. [12] presented viscosity data that were acquired from several experiments by using a cylindrical Couette

Table 1c
Results from durability experiments

Batch number	MPCM size range (μm)	Total time of durability test[a] (h)	% of broken microcapsules (%)	Slurry velocity (m/s)	Accumulative circulation times
1	90–150	9.7	15.5	0.6–2.4	700
2	70–260	5	16	0.6	400
3	2–10	7	0[b]	0.6–2.4	1200

[a] Total time includes cumulative results for the same batch at low and high mass fraction.
[b] No significant amount of free or released tetradecane was detected (within a 2% margin of error).

viscometer and pressure drop measurements. In that study, the apparent viscosity of MPCM slurry clearly showed a Newtonian fluid behavior when a 1% anionic surfactant was used. A later study [2] showed that the relative viscosity of MPCM slurry was fairly independent of temperature, suggesting a strong correlation with changes in the viscosity of pure water.

For this study, absolute viscosity was measured to be able to calculate and predict the effective Reynolds number and the associated turbulence range. As a result, an experimental heat transfer test loop was designed and constructed to measure heat transfer rates. A temperature-controlled concentric viscometer was used to determine the apparent viscosity of MPCM slurry. The device measures the viscosity of a sample by measuring the torque exerted by the fluid against a rotating cylinder. A Brookfield viscometer, model LVT with a microliter (UL) adapter was used to measure the viscosity of the MPCM slurry. For temperature control, the container or UL adapter was connected to a water bath that circulated water at a fixed temperature. A solution of laboratory-grade propylene glycol–water mixture at 34.6% and known viscosity values was prepared to calibrate the viscometer. The viscometer was calibrated at different temperatures and spindle rotational velocities after the system had reached a constant temperature for at least 30 min. It was determined that the viscometer was within a 1% margin of error, which supports the viscometer manufacturer claim.

The viscosity of MPCM samples at different mass fractions was measured at 12, 30, and 60 rpm to determine if the slurry behaved as a Newtonian fluid. Each sample was in the UL adapter for 30 min and stirred magnetically to make sure all the microcapsules were in suspension before measuring viscosity. Three measurements were taken for every sample. The mass fraction of each sample was determined by taking about three 20 μl samples of MPCM slurry from the UL adapter. Each 20 μl sample was dried to determine its water content and mass fraction. Statistical analysis was used to determine which set of data points was suitable for further analysis. Fig. 1d shows the statistically significant viscosity results.

Fig. 1d shows that the relative viscosity of MPCM slurry (size: 2–10 μm) seems to be independent of temperature regardless of mass fraction, reaffirming the results presented by Yamagishi et al. [2]. Relative viscosity is defined as the ratio between the apparent viscosity of MPCM slurry to that of water at a given temperature. Thomas [31] analyzed several experimental results reported earlier and noted lower relative viscosity for the same mass fraction shown in Fig. 1d. However, Yamagishi et al. [2] also found that MPCM slurry has a higher relative viscosity than indicated in the data collected and analyzed by Thomas [32] and comparable to the data depicted in Fig. 1d, suggesting that microcapsule shape and rigidity may be playing a role in increasing relative viscosity [2]. However, it is not clear if particle rigidity or shape can explain the increased relative viscosity values. Further studies are necessary to determine what causes increased viscosity including the hydroscopic nature of the microcapsule wall and the tendency to attract surrounding water. The MPCM viscosity results also indicate that MPCM slurry behaves as a Newtonian fluid at least up to a mass fraction of 17.7%.

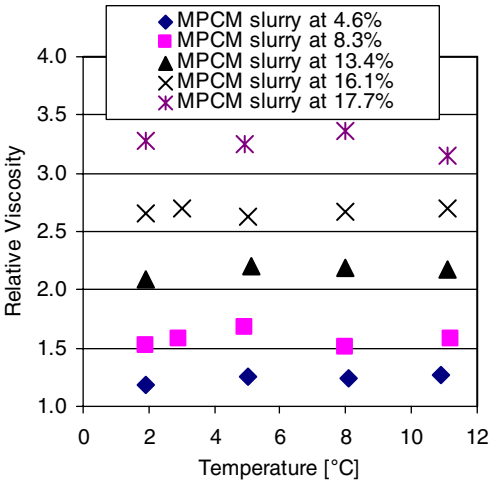

Fig. 1d. Relative viscosity of MPCM slurry as function of mass fraction and temperature.

The impact of higher viscosity at lower temperature and higher mass fraction should also be taken into consideration when selecting operating conditions or sizing equipment, because higher viscosity represents higher pumping power, lower turbulence, and lower overall thermal conductivity, which could reduce local heat transfer rates in the absence of a phase change process. The data depicted in Fig. 1d can also be used for thermal system simulations and to estimate level of turbulence in the slurry.

4. Microencapsulated phase change material slurry pressure drop and convective heat transfer characterization

4.1. Experimental system design

A heat transfer section was designed to measure the convective heat transfer and pressure drop of MPCM slurry before, during, and after the phase change material has undergone a solid-to-liquid transformation. To achieve fully turbulent conditions at different MPCM slurry mass fractions, the Reynolds number was calculated taking into account pipe diameter, fluid velocities between 0.6 and 2.4 m/s, and the measured slurry viscosity.

4.1.1. Experimental heat transfer section

A 12.2 m (40 feet) long heat transfer section was constructed and tested to be able to determine the convective heat transfer coefficient and pressure drop of MPCM slurry. The copper tubing length guaranteed a full phase change transition as well as hydrodynamic and thermal entry length requirements. The section consisted of eight 1.52-m (5 foot) long subsections made of 10.9 mm (3/8 in.) copper tubing.

Each subsection had a total of five thermocouples type T soldered to the outer surface at 30.5, 61, 76.2, 91.4 and 121.9 cm (12, 24, 30, 36, and 48 in.) from either end of the subsection. Each tubing subsection was then coated with plastic paint to minimize electrical conduction. A 24 gauge insulated nichrome wire was coiled around the copper tubing to provide constant heat flux. Each tubing subsection had three independent nichrome wire sections all connected in parallel. The entire heat transfer section consisted of 24 independent nichrome wire sections all connected in parallel to ensure constant heat flux. Additional nichrome wire was added as external resistance as needed to balance the electric load (voltage-squared/resistance or current-squared * resistance) so each section could provide the same overall heat flux. Additional nichrome wire was connected by using ceramic terminal blocks that were not in direct contact with the tubing sections. A thick layer of fiberglass insulation was used to thermally insulate each subsection.

The subsections were connected by using PVC coupling and plastic tubing to minimize axial heat conduction. Thermocouples were placed between each subsection to measure the fluid temperature. A strip of twisted copper sheet was inserted in the PVC coupling to ensure "mixing cup" or well mixed temperature conditions. All the sections were aligned horizontally by using a laser level. A Moyno Progressing cavity pump was used to pump the slurry through the system. An Omega magnetic flowmeter was used to measure fluid velocity to an accuracy of 0.5%. The performance of the magnetic flowmeter was validated by performing a simple bucket-watch experiment with water. Three Cole Parmer pressure differential transducers were used to measure pressure drop. Each pressure transducer could detect up to 17.2 kPa (2.5 psig) with 0.25% accuracy of the full range. Two alternating current variable voltage transformers (Variacs) were used as power supplies. Each could provide from 0 to 208 V. For data logging, an Agilent Data Logger (34970A Data Acquisition/Switch Unit) with three multiplexer cards was used to record temperature and pressure drop. An independent power meter was used to measure total power consumption as well as current and voltage delivered by each transformer.

The last subsection of the heat transfer loop was interchangeable, which allowed for changes in pipe diameter or tubing type. In addition to using 10.9 mm (3/8-in.) copper tubing, soft copper and enhanced copper tubing of 8 mm was also used to determine the impact of $d_{\text{pipe}}/d_{\text{particle}}$ ratio and tubing roughness (or enhancement) on the heat transfer process. The enhanced tubing section consisted of helical microfins of 200 μm in height and width, with about 60 microfins around the circumference. The orientation of the microfins with respect to the longitudinal axis was 18°.

A water-ice bath was used as the cooling medium to force the microencapsulated phase change material to undergo a liquid-to-solid transformation. Two compact heat exchangers were used to provide enough heat transfer area to ensure full phase change. A simple schematic of the entire system is shown in Fig. 2a.

Calibration of the thermocouples was performed in situ. Based on the recorded and scanned temperature values, appropriate and acceptable offset and gain values were determined for each thermocouple, all within 10% of the non-calibrated settings. Several heat transfer experiments with plain water were conducted to validate the calibration procedures. The following sections explain in details the validation procedure and results.

4.2. Pressure drop measurement – water test

Pressure drop data was analyzed and compared with the Darcy-Weisbach Eq. (2), the Colebrook correlation for friction factor (3), and the steady-flow energy Eq. (4):

Darcy-Weisbach:

$$h_{\text{f}} = f\frac{L}{d}\frac{V^2}{2g},\ \text{m} \tag{2}$$

where f, L, d, V, and g are the friction factor, pipe length, pipe diameter, fluid velocity, and gravitational constant, respectively.

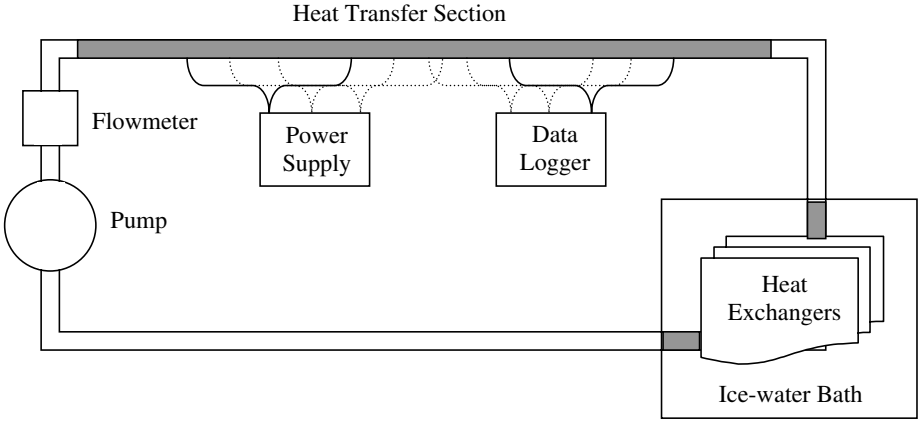

Fig. 2a. Schematic of heat transfer loop.

Colebrook equation [33]:

$$\frac{1}{\sqrt{f}} = 1.14 + 2\log\left(\frac{d}{\varepsilon}\right) - 2\log\left[1 + \frac{9.3}{Re\left(\frac{\varepsilon}{d}\right)\sqrt{f}}\right];$$

$$\text{for } Re > 3000 \tag{3}$$

where f, ε/d, and Re are the friction factor, relative roughness, and Reynolds number, respectively.

Steady-flow energy equation (for horizontal pipes):

$$h_f = \frac{\Delta P}{\rho g} \tag{4}$$

where h_f, ΔP, ρ, and g are friction head loss, pressure drop, fluid density, gravitational constant, respectively.

Three wet-to-wet differential pressure transducers from Cole-Parmer were used to measure pressure drop at several velocities and slurry concentrations. The pressure transducers were calibrated using the specifications provided by the manufacturer. The calibration results were validated by using plain water. The pressure transducers generated a current signal which was converted to pressure units by the data acquisition unit (Agilent unit).

The validation results indicate good agreement with the calculated results for the same flow conditions assuming smooth tubing surface (within 8% relative error). The results from the pressure drop test using enhanced tubing were compared with simulated and calculated results based on the Colebrook equation. Simulated results were based on the standard roughness factor (ε) for copper tubing and 0.2 mm for the enhanced tubing to take into account the microfin enhancement size.

Pressure drop experiments [13] suggest that a roughness factor value for an 8 mm enhanced tubing section falls between the characteristic value for smooth copper tubing and a roughness value of 0.2 mm. As per the Colebrook equations, a roughness factor of 0.1 mm seems to reasonably match the pressure drop profile of the enhanced tubing [13].

4.3. MPCM slurry pressure drop test

Several pressure tests were conducted to determine pressure drop of MPCM slurry at two mass fractions. Pressure drop data were collected when the slurry reached steady-state temperature and flow conditions. Fig. 2b shows the results from a pressure drop test at low mass fraction ($5.9 \pm 0.4\%$). Fig. 2b also shows a simulated pressure drop profile for water based on the Colebrook equation at the same flow conditions as for the MPCM slurry. The results indicate that pressure drop increases slightly when MPCM particles are used, but not significantly enough to affect pumping power.

Fig. 2c shows pressure drop results at 5.9% ($\pm 0.4\%$) mass fraction when 8 mm smooth, and 8 mm enhanced tubing sections were tested. Pressure drop for MPCM slurry is lower than a simulated pressure drop profile for water based on the Colebrook equation and an 8 mm smooth tubing section. Fig. 2c also reveals that enhanced and smooth tubing sections display similar pressure drop behavior and magnitude. The plot also shows that the experimental pressure drop for water is greater than for the MPCM slurry at 5.9% mass fraction when enhanced tubing was tested. The results may suggest that a small amount of microcapsules ruptured and released phase change material into the carrier fluid, creating favorable conditions for a drag-reducing effect [34]. Samples were taken and examined to look for broken capsules or released tetradecane within a 2% margin of error. No significant amount of tetradecane could be detected and micrographs could not reveal the presence of broken capsules. It is plausible that the microencapsulation process produced a small

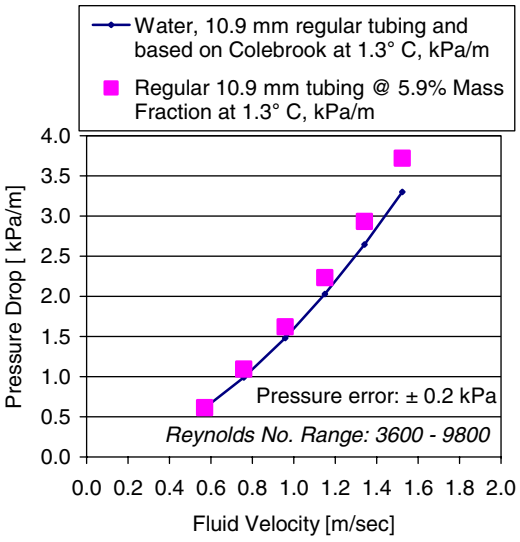

Fig. 2b. Pressure drop of MPCM slurry at 5.9% mass fraction, 10.9 mm regular tubing.

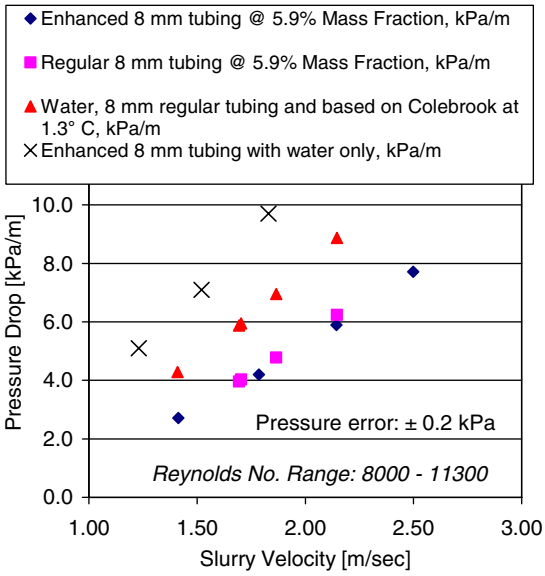

Fig. 2c. Pressure drop of MPCM slurry at 5.9% mass fraction, 8 mm regular and 8 mm enhanced tubing.

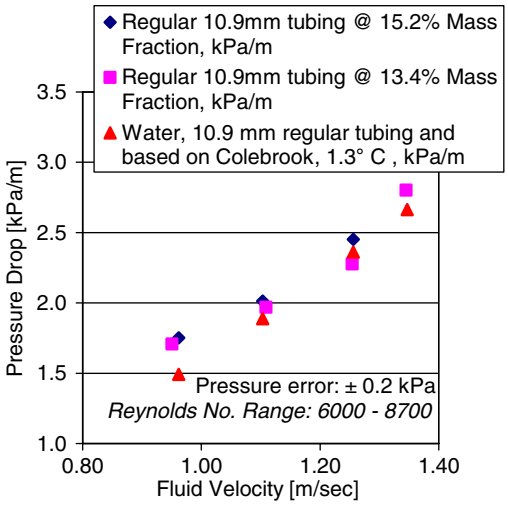

Fig. 3a. Pressure drop of MPCM slurry at 13.4% and 15.2% mass fraction, 10.9 mm smooth tubing.

amount of aggregates (not fully formed capsules) that were prone to early breakage. Visual inspection of the entire batch did not reveal any significant amount of free tetradecane at the surface of a 10-litre container, so only a small amount of free tetradecane might have remained in solution. It is plausible that a small amount of free tetradecane could have cancelled any drag effect associated with the enhanced surface [23]. Fossa and Tagliafico [23] observed significant drag reduction or friction coefficient reduction (5–25%) when long-chain molecules in concentrations from 5 to 40 ppm were tested in combination with tubing that had helical groove enhancements.

Fig. 3a shows pressure drop results at 13.4% and 15.2% (±0.4%) mass fractions for a 10.9 mm smooth tubing section. Pressure drop for MPCM slurry at 15.2% mass fraction is relatively higher than a simulated pressure drop profile for water based on the Colebrook equation when a 10.9 mm tubing section was used. The results are consistent with the pressure drop results seen at low mass fractions, suggesting that the same mechanisms are also in play at higher mass fractions.

As seen in all cases, pressure drop does not increase with particle loading, suggesting that a drag-reducing effect could play a major role in reducing friction and pressure drop. As noted earlier, small microcapsules (2–10 μm) suppress turbulence [35] and have a considerable impact on pressure drop too. The Reynolds number range is shown in each figure and is based on the apparent viscosity of the MPCM slurry at the specified mass fraction.

4.4. Convective heat transfer coefficient measurement – water test

Water heat transfer tests were conducted and temperature data were collected by using thermocouples and a sensitive data acquisition system as described above. The amount of power for each section was measured to determine each section's associated heat flux. Each section experimental heat transfer coefficient was calculated based on the following relation:

$$h = \frac{q''}{T_{\text{wall}} - T_{\text{bulk}}} \tag{5}$$

where q'', T_{wall}, and T_{bulk} are the wall heat flux, wall temperature, and bulk fluid temperatures respectively. The experimental convective heat transfer coefficient was analyzed and compared with the Gnielinski correlation:

$$Nu_{\text{d}} = \frac{\left(\frac{f}{8}\right)(Re_{\text{d}} - 1000)Pr}{1 + 12.7\left(\frac{f}{8}\right)^{1/2}(Pr^{2/3} - 1)} \tag{6}$$

where Nu_{d}, f, Re_{d}, and Pr are the Nusselt number, friction factor, Reynolds, and Prandtl numbers, respectively. The Gnielinski correlation is valid for $0.5 < Pr < 2000$ and $3{,}000 < Re < 5 \times 10^6$, and takes into account the friction factor. Other correlations, including the Dittus-Boelter and Sieder and Tate correlations, are valid when the Reynolds number is greater than 10,000.

The following equation is used to determine the convective heat transfer coefficient based on the Nusselt number:

$$h = Nu_{\text{d}}\frac{k}{d} \tag{7}$$

where h, Nu_{d}, k, and d are the convective heat transfer coefficient, Nusselt number, fluid thermal conductivity determined at the bulk fluid temperature, and pipe diameter, respectively.

The validation heat transfer experiments indicate good agreement with the Gnielinski correlation evaluated at the same conditions and fluid properties. Uncertainty analysis revealed that the compounded error was less than ±8.0%. Using the Gnielinski correlation for smooth tubing under identical conditions, fluid properties, and tubing characteristics, the enhanced tubing enhancement factor is 1.17. The enhancement factor is defined as follows:

$$\text{Enhancement\_Factor} = \frac{h_{\text{enhanced}}}{h_{\text{smooth}}} \tag{8}$$

where h_{enhanced}, and h_{smooth} are the heat transfer coefficients for enhanced tubing and smooth tubing, respectively. The experimental heat transfer coefficient for the enhanced tubing is based on a diameter of 8 mm (smooth). However, the defined enhancement factor does not reflect the enhanced tubing actual heat transfer area. The enhanced tubing has approximately 1.6 times the amount of surface area of smooth tubing for the same diameter.

After taking into account the enhanced tubing additional surface area, it can be concluded that that the microfins or enhancements on the tubing inner surface curtail the heat transfer process but make up the difference by providing more surface area for heat transfer. This suggests that enhancements affect the momentum transfer from the wall to the bulk fluid. Zukauskas [36] studied the impact of enhancements in detail and concluded that the height of the enhancement should only be high enough to disturb

the viscous sublayer in liquids. Zukauskas [36] defined a dimensionless roughness height, k^+, which is defined as follows:

$$k^+ = \frac{ku_*}{v} \tag{9}$$

where k^+, k, u^*, and v are the dimensionless roughness, roughness height, friction velocity, and kinematic viscosity, respectively.

Previous experiments [35] showed that k^+ should fall between 5 and 70 for improving the heat transfer rate; otherwise the enhancement could be ineffective. In the case of water at 1.76 m/s, k^+ is about 0.25, which suggests that a higher enhancement is advisable as long as the pressure drop does not increase drastically.

4.5. MPCM slurry heat transfer test

Several heat transfer experiments were conducted to determine the convective heat transfer coefficient of MPCM slurry at high and low mass fractions. Temperature and power readings necessary for the calculation of the heat transfer coefficient were taken when the slurry inlet temperature reached a steady state value of approximately 1.8 °C or less. When the inlet temperature reached 1.8 °C or less, a full liquid-to-solid transformation of the phase change material was assumed. Simple energy balance calculations based on temperature, power, and flow-meter readings were performed to verify that the MPCM slurry sensible and latent heat capacities match the energy input within a margin of error of 10% or less.

Fig. 3b shows the experimental temperature profiles (temperature vs. tubing length) for several heat transfer tests of MPCM slurry at 7.0% (±0.4%) when the slurry velocity was varied between 0.64 and 1.08 m/s. Fig. 3b also shows that a 40% experimental heat capacity enhancement can be obtained when assuming identical flow conditions (initial temperature and flow rate) when using plain water. Three distinct temperature regions are shown in Fig. 3b including before-melting (BM), during-melting (DM), and after-melting (AM). In the DM region, where most of the MPCM melting process takes places, the slurry temperature increases slightly even with significant constant heat flux. The melting process of tetradecane helps maintain a lower temperature in the carrier fluid (water), which in turn allows heat transfer to occur at lower temperatures than normal.

Fig. 3b also shows that the MPCM slurry temperature profiles display three slope changes at approximately 5.5 °C. Under ideal circumstances, the temperature gradient for the DM region should be close to zero during the phase change process. However, the experimental data reveal a slope greater than zero because not all the microcapsules could undergo phase change at the same time. Microcapsules closer to the tube wall undergo phase change first, affecting the slurry bulk temperature as they exchange energy with the surrounding fluid and other microcapsules that have undergone only partial phase change or none at all.

Figs. 3c and 3d show the experimental heat transfer coefficient for several heat transfer tests of MPCM slurry at 7.0% (±0.4%) within a 7% margin of error. Fig. 3c shows that the convective heat transfer coefficient (h) peaks at approximately 5.0 m. By comparing Figs. 3b and 3c, it is evident that h reaches its maximum value at approximately 5.5 °C or near the melting point of tetradecane. Also, the additional heat capacity available during the phase change process (DM region) enhances the heat transfer coefficient as shown in Figs. 3c and 3d and is in line with the notion that at a higher heat capacity or Prandtl number, the convective heat transfer coefficient increases accordingly [10]. It is also evident that h increases significantly with fluid velocity because of greater momentum transfer at high velocities. However, the heat transfer coefficient for MPCM slurry is lower than that for pure water at the same velocities, suggesting that MPCM particles attenuate turbulence and momentum transfer. It is known that particle

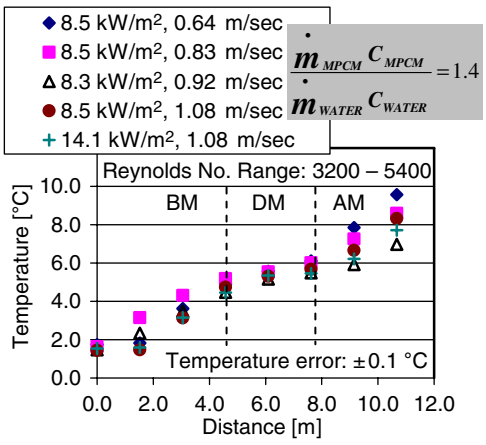

Fig. 3b. Heat transfer coefficient of MPCM slurry at 7.0%, 10.9 mm regular tubing.

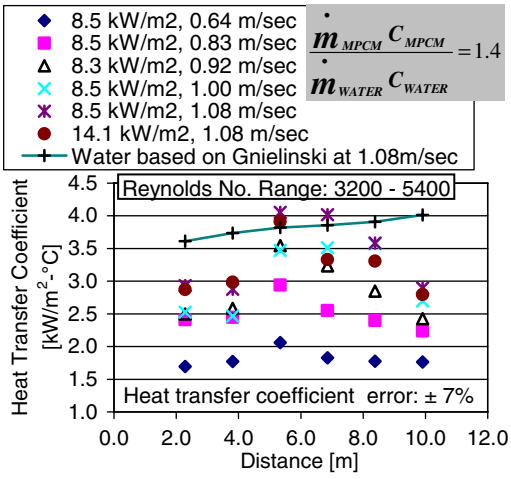

Fig. 3c. Temperature profile for MPCM slurry at 7.0%, 10.9 mm smooth tubing.

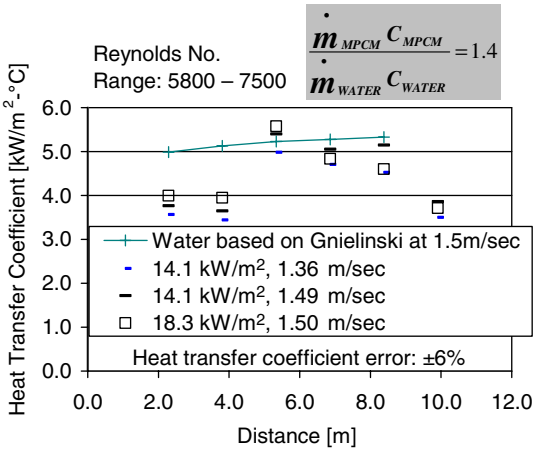

Fig. 3d. Heat transfer coefficient of MPCM slurry at 7.0%, 10.9 mm regular tubing.

size can either enhance or suppress turbulence. Experimental data [35] suggest that small particles such as the ones used here (2–10 μm), and whose relation to the characteristic fluid length scale (d_p/L_e) is less than 0.1, have shown considerable turbulence suppression and therefore, lower momentum transfer.

Fig. 4a shows the MPCM slurry temperature profile at a mass fraction of 16.5% in a 10.9 mm heat transfer section. Fig. 4a shows that at a higher heat flux (16.3 kW/m^2) and higher velocity (1.21 m/s), the MPCM slurry exhibits noticeable changes in temperature gradient. Fig. 4b shows the heat transfer coefficient for MPCM slurry under same conditions as in Fig. 4a, which is lower than that for plain water under the same conditions. This indicates that MPCM slurry at higher mass fractions (higher apparent viscosity) results in lower turbulence, which curtails heat transfer from the wall to the bulk fluid. On the other hand, the experimental heat capacity (70%) is considerably larger than that of water under the same conditions. To take full

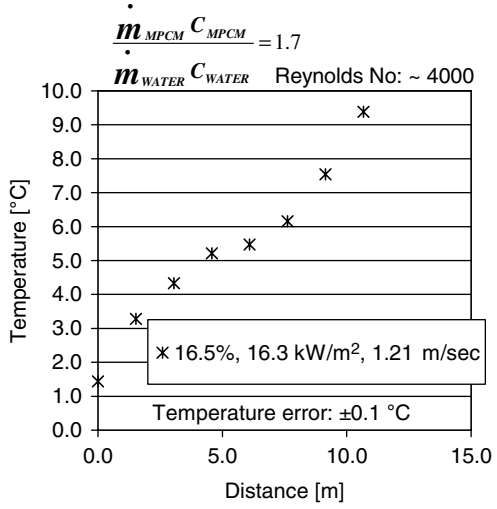

Fig. 4a. Temperature profile for MPCM slurry at 16.5%, 10.9 mm smooth tubing.

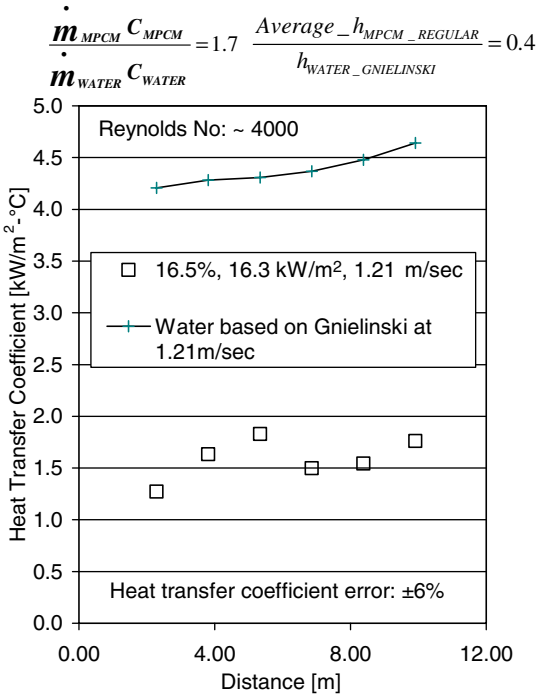

Fig. 4b. Heat transfer coefficient of MPCM slurry at 16.5%, 10.9 mm smooth tubing.

advantage of the MPCM slurry heat capacity, enhanced tubing that provides 60% more heat transfer area was also tested.

Fig. 4c shows the heat transfer coefficient of MPCM slurry at 7.0% mass fraction when smooth and enhanced 8 mm tubing sections were used. The experimental data suggest that enhanced tubing does improve the heat transfer process at low mass fraction, as indicated by the enhancement factor shown in Fig. 4c. However, plain water still has a greater heat transfer coefficient under

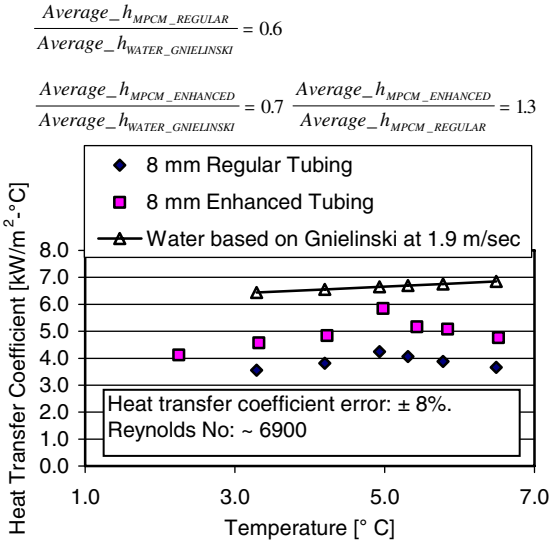

Fig. 4c. Heat transfer coefficient of MPCM slurry at 7.0%, 8 mm regular and 8 mm enhanced tubing.

identical conditions. This suggests two courses of action for future studies: greater tubing enhancement or thermal conductivity enhancement of the heat transfer fluid [13]. The latter is currently being considered by the authors.

Fig. 4d shows the heat transfer coefficient of MPCM slurry at 12.0% mass fraction when a 8 mm smooth tubing section was used. As in the case of the 10.9 mm tubing section, the heat transfer enhancement is 0.4, which can be attributed to lower turbulence at higher mass fractions and smaller tubing size. Fig. 5 shows that h decreases considerably at higher mass fractions in enhanced tubing [13]. This may suggest that a larger pipe diameter and a different type of enhancement could still enhance the MPCM slurry heat transfer performance at high mass fractions.

Another important goal of the heat transfer experiments was to determine the percentage (ϕ) of particles that underwent phase change before the bulk fluid reached the melting point of tetradecane. Energy balance calculations were performed using Eq. (10) and taking into account slurry temperature rise (ΔT) and heat transfer section length (L) to determine ϕ. The left and right sides of Eq. (10) represent the heat transfer through the tube wall and MPCM slurry heat rate, respectively.

$$q''_{\mathrm{w}}(\pi d)L = (1-\phi)[\dot{m}\Delta T((1-MF)c_{p\_\mathrm{water}} + (\mathrm{MF})c_{p\_\mathrm{MPCM}})] + \phi[\dot{m}(\mathrm{MF})\lambda_{\mathrm{MPCM}}] \qquad (10)$$

By also taking into account MPCM slurry mass flow rate, heat flux, and mass fraction, the value of ϕ for each heat transfer experiment was calculated [13]. In the before-melting (BM) region, ϕ represents the average percentage of MPCM particles transferring from the core fluid to the viscous layer region, where the wall layer fluid is at a sufficiently high temperature to cause phase change of the MPCM particles entering that region. Alvarado [13] observed that ϕ increases with heat flux (or a greater thermal gradient near the surface) and flow rate (or higher momentum transfer from the wall to the core fluid). However, the heat transfer experiments revealed that slurry velocity (momentum transfer) has a greater impact on ϕ than heat flux (thermal gradient near the tube wall) [13]. Also, significant MPCM particle migration can be observed when both heat flux and slurry velocities are increased considerably [13]. This observation can be explained by the increased level of turbulence and greater thermal gradient near the tube wall.

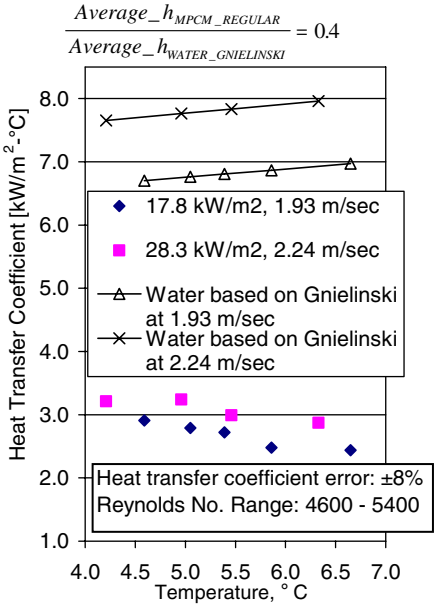

Fig. 4d. Heat transfer coefficient ofMPCM slurry at 12.0%, 8 mm regular tubing.

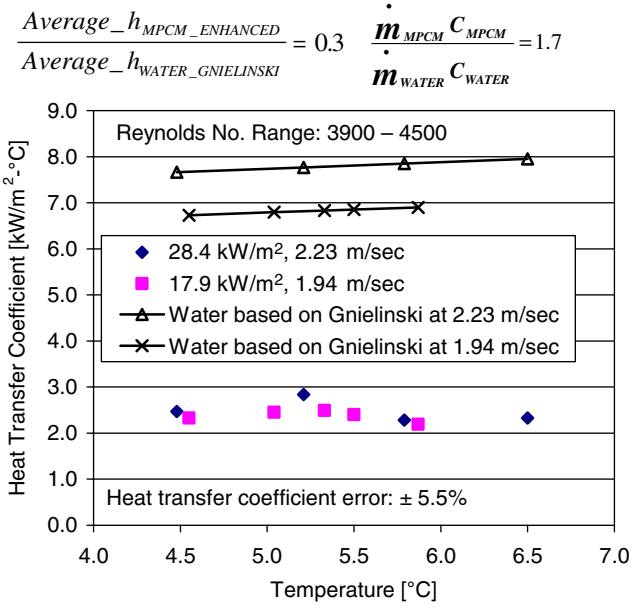

Fig. 5. Heat transfer coefficient of MPCM slurry at 15.2%, 8 mm enhanced tubing.

5. Conclusions

The experimental data presented in this paper show that MPCM slurry can provide considerable heat capacity in heat transfer applications. Other important observations and conclusions are as follows:

- Thermal characterization of MPCM slurry by using DSC reveals that supercooling of the phase change material can be suppressed significantly by incorporating the right amount and type of nucleating agent.
- MPCM slurries exhibit a Newtonian-like behavior at mass fractions below 17.7%, and the relative viscosity is independent of temperature.
- Microcapsules become durable and impact-resistant when smaller than 10 μm.
- Pressure drop experiments revealed a possible drag-reducing effect, which should be investigated further.
- Heat transfer experiments showed that the heat capacity enhancements are considerable, even at low mass fractions.

- MPCM slurry heat transfer coefficients are typically lower than that of water at the same velocities. Use of a different type of enhanced tubing or enhancement of MPCM slurry thermal conductivity could improve heat transfer beyond the current levels.
- The heat transfer coefficient increases considerably during the phase change process.
- Enhanced surface tubing is more advantageous at low mass fraction than at a high mass fraction.
- Particle migration toward the near-wall region before, during and after the bulk fluid reaches the phase change material melting point is affected by slurry velocity more significantly than by heat flux.

Future studies should focus on the identification of durable capsule materials able to resist microbial action and harsh environments. Greater and other types of enhanced tubing should be considered to determine if the MPCM slurry heat transfer coefficient can be increased at higher mass fraction. Also, ways to increase the thermal conductivity of heat transfer fluids should be identified and studied carefully.

Acknowledgements

The authors would like to express their deepest thanks to Professor Shelly Schmidt and Dr. Dawn Bohn of the Food Science Department at the University of Illinois; and Mr. Vince Hock, Dr. Don Cropek, Pat Kemme, Jose Parrilla, Eric Crowley, Angelo DeGuzman, Bill Gordon, and Moeliere Vilceus of the US Army Corps of Engineers Construction Engineering Research Laboratory. I am also grateful for the technical support and expertise provided by Professor Curt Thies of Thies Technology, whose know-how was indispensable during the execution of the project.

References

[1] H. Bo, M. Gustafsson, F. Setterwall, Tetradecane and hexadecane binary mixtures as phase change materials for cool storage in district cooling systems, Energy 24 (1999) 1015–1028.
[2] Y. Yamagishi, H. Takeuchi, A.T. Pyatenko, N. Kayukawa, Characteristics of MPCM slurry as a heat transfer fluid, AIChE J. 45 (1999) 696–707.
[3] E. Choi, Forced convection heat transfer with water and phase-change material slurries: turbulent flow in circular tube, Ph.D. Thesis, Drexel University, Philadelphia, PA, 1993.
[4] J. Bellas, I. Chaer, S.A. Tassou, Heat transfer and pressure drop of ice slurries in plate heat exchangers, Appl. Thermal Eng. 22 (2002) 721–732.
[5] E. Choi, Y.I. Cho, H.G. Lorsch, Forced convection heat transfer with phase-change-material slurries: turbulent flow in a circular tube, Int. J. Heat Mass Transfer 37 (2) (1994) 207–215.
[6] K. Chen, M.M. Chen, Analytical and experimental investigation of the convective heat transfer of phase-change slurry flows, J. Heat Transfer (1984) 496–501.
[7] E. Choi, Y.I. Cho, H.G. Lorsch, Effects of emulsifier on particle size of a phase change material in a mixture with water, Int. Commun. Heat Mass Transfer 18 (1991) 759–766.
[8] J.P. Dumas, M. Krichi, M. Strub, Y. Zeraouli, Models for the heat transfer during the transformations inside an emulsion I. Crystallizations of the undercooled droplets, Int. J. Heat Mass Transfer 37 (5) (1994) 737–746.
[9] B. He, F. Setterwall, Technical grade paraffin waxes as phase change materials for cool thermal storage and cool storage systems capital cost estimation, Energy Convers. Manage. 43 (2002) 1709–1723.
[10] K.E. Kasza, M.M. Chen, Improvement of the performance of solar energy waste heat utilization systems by using phase-change slurry as an enhanced heat transfer storage fluid, J. Solar Energy Eng. 107 (1985) 229–236.
[11] S.K. Roy, S. Sengupta, An evaluation of phase change microcapsules for use in enhanced heat transfer fluids, Int. Commun. Heat Mass Transfer 18 (1991) 495–507.
[12] Y. Yamagishi, T. Sugeno, T. Ishige, H. Takeuchi, A.T. Pyatenko, An evaluation of microencapsulated PCM for use in cold energy transportation medium, in: Proceedings of the Intersociety of Energy Conversion Engineering Conference, IEEE, 1996, pp. 2077–2083.
[13] J.L. Alvarado, Thermal performance of microencapsulated phase change material slurry, Ph.D. Thesis, University of Illinois at Urbana-Champaign, Urbana, IL, 2004.
[14] V. Vand, Viscosity of solutions and suspensions, J. Phys. Colloid Chem. 52 (1948) 277–321.
[15] T. Ohtsubo, S. Tsuda, K. Tsuji, A study of the physical strength of fenitrothion microcapsules, Polymer 32 (13) (1991) 2395–2399.
[16] M.S. Goel, S.K. Roy, S. Sengupta, Laminar forced convection heat transfer in microcapsulated phase change material suspensions, Int. J. Heat Mass Transfer 37 (4) (1994) 593–604.
[17] S.K. Roy, B.L. Avanic, Laminar forced convection heat transfer with phase change material emulsions, Int. Commun. Heat Mass Transfer 24 (5) (1997) 653–662.
[18] R.A. Gore, C.T. Crowe, Turbulence in slurry pipe flow. Cavitation and multiphase flow forum, Proc. ASME Fluids Eng. Div. 98 (1990) 175–178.
[19] G. Hetsroni, Particles-turbulence interaction, Int. J. Multiphase Flow 15 (5) (1989) 735–746.
[20] X. Hu, Y. Zhang, Novel insight and numerical analysis of convective heat transfer enhancement with microencapsulated phase change material slurries: laminar flow in a circular tube with constant heat flux, Int. J. Heat Mass Transfer 45 (2002) 3163–3172.
[21] Y. Zhang, X. Xu, X. Wang, Theoretical analysis of convective heat transfer enhancement of microencapsulated phase change material slurries, Heat Mass Transfer 40 (2003) 59–66.
[22] A. Durmus, A. Durmus, M. Esen, Investigation of heat transfer and pressure drop in a concentric heat exchanger with snail entrance, Appl. Thermal Eng. 22 (2002) 321–332.
[23] M. Fossa, L.A. Tagliafico, Experimental heat transfer of drag-reducing polymer solutions in enhanced surface heat exchangers, Exp. Thermal Fluid Sci. 10 (1995) 221–228.
[24] Q. Liao, M.D. Xin, Augmentation of convective heat transfer inside tubes with three-dimensional internal extended surfaces and twisted-tape inserts, Chem. Eng. J. 78 (2000) 95–105.
[25] M.M. Clark, Transport Modeling for Environmental Engineers and Scientists, John Wiley and Sons, New York, 1996.
[26] E.L. Charsley, S.B. Warrington, Thermal Analysis: Techniques and Applications, Thomas Graham House, Cambridge, 1992.
[27] T. Hatakeyama, F.X. Quinn, Thermal Analysis: Fundamentals and Applications to Polymer Science, John Wiley & Sons, New York, NY, 1994.
[28] R.F. Speyer, Thermal Analysis of Materials, Marcel Dekker Inc., New York, NY, 1994.
[29] J.L. Alvarado, C. Marsh, C. Sohn, V. Hock, G. Phetteplace, T. Newell, Characterization of supercooling suppression of microencapsulated phase change material by using DSC, J. Thermal Anal. Calorimetry 86 (2006) 505–509.
[30] R. Montenegro, M. Antonietti, Y. Mastai, K. Landfester, Crystallization in miniemulsion droplets, J. Phys. Chem. 107 (2003) 5088–5094.

[31] R. Montenegro, K. Landfester, Metastable and stable morphologies during crystallization of alkanes in miniemulsion droplets, Langmuir 19 (2003) 5996–6003.
[32] D.G. Thomas, Transport characteristics of suspension: VIII. A note on the viscosity of Newtonian suspensions of uniform spherical particles, J. Colloid Sci. 20 (1965) 267–277.
[33] American Society of Heating, Refrigeration and Air Conditioning Engineers (ASHRAE), ASHRAE Handbook Fundamentals, Chapter 38, 2001.
[34] M. Kostic, On turbulent drag and heat transfer reduction phenomena and laminar heat transfer enhancement in non-circular duct flow of certain non-Newtonian fluids, Int. J. Heat Mass Transfer 37 (suppl. 1) (1994) 133–147.
[35] C. Crowe, M. Sommerfeld, Y. Tsuji, Multiphase Flows with Droplets and Particles, CRC Press, Boca Raton, FL, 1998.
[36] A. Zukauskas, Enhancement of forced convection heat transfer in viscous fluid flows, Int. J. Heat Mass Transfer 37 (suppl.1) (1994) 207–212.